***Schizosaccharomyces versatilis* represents a distinct evolutionary lineage.**

Graham J Etherington [1]*, Elisa Gomez Gil [2,3], Wilfried Haerty [1], Snezhana Oliferenko, [2,3] and Conrad A. Nieduszynski [1,4]*

Running title: *S. versatilis* species status.

[1]The Earlham Institute, Norwich Research Park, Norwich, NR4 7UZ, United Kingdom
[2]The Francis Crick Institute, 1 Midland Road, London, NW1 1AT, UK
[3]Randall Centre for Cell and Molecular Biophysics, School of Basic and Medical Biosciences, King's College London, London, SE1 1UL, UK
[4]School of Biological Sciences, University of East Anglia, Norwich, NR4 7TU, United Kingdom

*Corresponding authors: graham.etherington@earlham.ac.uk
Conrad.Nieduszynski@earlham.ac.uk

ORCIDs:
Graham J Etherington - 0000-0002-5003-1425
Elisa Gómez-Gil - 0000-0001-9157-2028
Wilfried Haerty - 0000-0003-0111-191X
Snezhana Oliferenko - 0000-0002-8138-6851
Conrad Nieduszynski - 0000-0003-2001-076X

Keywords: Fission yeast, Schizosaccharomyces versatilis, evolution, taxonomy, adaptation.

Take-away:

- The taxonomic status of *Schizosaccharomyces versatilis* is addressed.
- *S. versatilis* diverged from *S. japonicus* around 25 million years ago.
- *S. versatilis* does not produce viable progeny in crosses with *S. japonicus.*
- *S. versatilis* has a reciprocal translocation between chromosomes 1 and 2.
- The Gene Ontology terms for genes in the translocations are enriched for terms connected to "metabolism" and "cellular assembly".

Abstract

The fission yeast species *Schizosaccharomyces japonicus* is currently divided into two variants – *S. japonicus* var. *japonicus* and *S. japonicus* var. *versatilis*. Here we examine the var. *versatilis* isolate CBS5679. The CBS5679 genome shows 88% identity to the reference genome of *S. japonicus* var. *japonicus* at the coding sequence level, with phylogenetic analyses suggesting that it has split from the *S. japonicus* lineage 25 million years ago. The CBS5679 genome contains a reciprocal translocation between chromosomes 1 and 2, together with several large inversions. The products of genes linked to the major translocation are associated with "metabolism" and "cellular assembly" ontology terms. We further show that CBS5679 does not generate viable progeny with the reference strain of *S. japonicus*. Although CBS5679 shares closer similarity to the "type" strain of var. *versatilis* as compared to S. *japonicus*, it is not identical to the type strain, suggesting population structure within var. *versatilis*. We recommend that the taxonomic status of *S. japonicus* var. *versatilis* is raised, with it being treated as a separate species, *Schizosaccharomyces versatilis*.

Introduction

Fission yeasts are a genus of symmetrically dividing pill-shaped yeasts within the Taphrinomycotina subdivision of Ascomycota fungi (Kurtzman & Sugiyama, 2015; Liu et al., 2009; Sugiyama, Hosaka, & Suh, 2006). Whilst budding yeast, another class of Ascomycota yeasts, are taxonomically diverse, containing numerous genera (including the model organism *Saccharomyces cerevisiae*), Schizosaccharomycetes contain only one genus – *Schizosaccharomyces*, which is currently subdivided into only six recognised species – *S. pombe*, *S. octosporus*, *S. cryophilus*, *S. osmophilus*, *S. lindneri* and *S. japonicus* (Michael Brysch-Herzberg, Jia, Seidel, Assali, & Du, 2022). *Schizosaccharomyces pombe* is a widely used model organism in diverse fields of molecular cellular biology research, which has provided fundamental insights into the regulation of cell growth and cell cycle, mitosis, meiosis, chromosome biology, RNA processing, epigenetics, cellular organization, polarity establishment and maintenance, cytoskeleton function, etc (Wood et al., 2002; Wood et al., 2012) . More recently, another fission yeast species, *Schizosaccharomyces japonicus*, has emerged both as a part of a powerful composite evolutionary cell biology model system used alongside *S. pombe* (Y. Gu, Yam, & Oliferenko, 2015; Makarova et al., 2016; Makarova et al., 2020; Yam, He, Zhang, Chiam, & Oliferenko, 2011) and as a valuable standalone model organism for the study of processes not apparent or tractable in other yeasts (Aoki et al., 2011; Chapman, Taglini, & Bayne, 2022; Furuya & Niki, 2010, 2012; Gomez-Gil et al., 2019; Y. Gu & Oliferenko, 2019; Kinnaer, Dudin, & Martin, 2019; Lee et al., 2020; Nozaki, Furuya, & Niki, 2018; Papp, Acs-Szabo, Batta, & Miklos, 2021; Pieper, Sprenger, Teis, & Oliferenko, 2020; Rutherford, Harris, Oliferenko, & Wood, 2022; Wang et al., 2021; Yam, Gu, & Oliferenko, 2013).

It has been proposed that *S. japonicus* has two variants (here denoted as 'var.'): *S. japonicus* var. *japonicus*, and *S. japonicus* var. *versatilis*. *S. japonicus* was first isolated in 1911 from Chapel Hill, USA (Michael Brysch-Herzberg et al., 2022), although not properly described until 1931 (Yukawa & Maki, 1931). *S. japonicus* var. *versatilis* was isolated in 1945 in Illinois, USA, from fermenting grape must (Wickerham & Duprat, 1945). Another strain of var. *versatilis* was discovered in the slime flux of the elm tree *Ulmus carpinifolia* at the University of California, Davis in 1960 (Phaff, Yoneyama, & CARMO-SOUSA, 1964). That strain has been deposited in the Westerdijk Institute collection as CBS5679. More recently, CBS5679 has been referred to as *S. japonicus* var. *japonicus* in yeast collections (e.g. https://www.dsmz.de/collection/catalogue/details/culture/DSM-70571, https://www.atcc.org/products/24256) and literature (Bouwknegt et al., 2021). In terms of taxonomic assignment, *S. japonicus* var. *versatilis* has a chequered history. Based on a variety of properties (e.g. iodine reaction of mature ascospores, cellular cytochrome spectra, prototrophic selection hybridisation, nDNA/nDNA optical reassociation, and ascospore shape), it has been split from and lumped with var. *japonicus* several times (Johannsen, 1981; Martini, 1991; Sipiczki, Kucsera, Ulaszewski, & Zsolt, 1982; Slooff, 1970; Yarrow, 1984).

Advances in whole genome sequencing and assembly methods have made it possible to sequence and assemble the relatively small genomes of yeast species cheaply and quickly. All known species of fission yeast have now been sequenced (M. Brysch-Herzberg et al., 2023; Jia et al., 2023; Rhind et al., 2011; Wood et al., 2002). More recently, the availability of low-cost long-read sequencing combined with advances in genome assembly algorithms has allowed for chromosome-scale telomere-to-telomere sequencing to become achievable even for the most complex genomes (Belser et al., 2021; Nurk et al., 2022).

Although genome-wide sequencing data is often generated for genome assembly, other questions can be addressed with the same data types. Recently, whole genome sequencing of the *S. japonicus* strain CBS5679 using long and short-reads was carried out in the course of inquiry into the mechanistic basis of anaerobic growth (Bouwknegt et al., 2021). We noticed that the sequencing data produced during this experiment differs greatly from the reference *S. japonicus* assembly (Rhind et al., 2011; Rutherford et al., 2022).

Here, we assemble the data generated by Bouwknegt (2021) and compare it to the reference assembly of *S. japonicus* and other *Schizosaccharomyces* species.

Materials and Methods

Genome assembly and quality control (QC)

We accessed publicly available DNA sequence data for *S. japonicus* CBS5679 generated under BioProject Accession PRJNA698797, which comprised Oxford Nanopore (ONT) long-reads (SRR15295841) and Illumina short-reads (SRR15295840) (Bouwknegt et al., 2021). We used Canu (Koren et al., 2017) to correct and trim the ONT reads and then generated an assembly using reads of >60 kb (resulting in 29,650 reads with an estimated coverage of 42x). We further polished the final assembly with the Illumina data using three rounds of Pilon polishing (Walker et al., 2014). We used BUSCO (v5.3.2) (Manni, Berkeley, Seppey, & Zdobnov, 2021) to identify the number of Ascomycota-specific single-copy orthologs recovered in the assembly. We then carried out repeat masking using a pipeline with RepeatModeler (Flynn et al., 2020) and RepeatMasker (Smit, Hubley, & Green, 2015; Tarailo-Graovac & Chen, 2009) and summarised the results using the ParseRM.pl script from the Parsing-RepeatMasker-Outputs tool (https://github.com/4ureliek/Parsing-RepeatMasker-Outputs).

Annotation

Liftoff (v1.5.1) (Shumate & Salzberg, 2020) was used to lift over the Ensembl Fungi *S. japonicus* (GCF_000149845.2_SJ5) annotation to CBS5679. Annotation of repeat content was generated using RepeatModeler v2.0.3 (Flynn et al., 2020) and RepeatMasker (v4.1.2-p1) (Smit et al., 2015; Tarailo-Graovac & Chen, 2009). tRNA loci were annotated using tRNAscan-SE (v2.0.12) (Chan, Lin, Mak, & Lowe, 2021). rRNA loci were annotated using barrnap (v0.9) (Seeman, 2018).

Comparison to S. japonicus

We used Nanopore reads from the type strain (FY16936) of *S. japonicus* (catalogue number ATCC10660) from ENA Project PRJEB63404 and included it in the following analyses. We also included a telomere-to-telomere genome assembly of *S. japonicus* (FY16936; GCA_956476325) to add resolution around the *japonicus-versatilis* analyses.

To compare sequence identity at the coding sequence (CDS) level between CBS5679 and *S. japonicus* FY16936, we downloaded the CDS sequences of *S. japonicus* from Ensembl Fungi (database version 109.2) and created a BLAST (v 2.7.1) database from the Nanopore reads of both FY16936 and CBS5679. We then used the Ensembl CDS sequences (4,892 in total) as the query sequences in separate blastn searches against the two sets of reads. We selected the best hit for each CDS and noted the percent identity, alignment length, number of mismatches, number of gaps opened, the e-value, and bit score for each hit and calculated the mean values for both FY16936 and CBS5679.

To compare sequence identity between CBS5679 and FY16936 assemblies and a previously published *S. japonicus* var. *versatilis* DNA sequence (Naehring, Kiefer, & Wolf, 1995) we

downloaded the Genbank sequence Z32848.1, encoding the 6.5 kb *S. japonicus* var. *versatilis* genes for 17S, 5.8S, and 25S ribosomal RNA (rRNA), which included the Internal Transcribed Spacer (ITS) 1 and ITS2. We generated BLAST databases for each genome and used Z32848.1 as the query sequence in a blastn search. We then identified the coordinates of the highest scoring hit from both CBS5679 and FY16936 assemblies and using the BEDTOOLS getfasta tools (v2.23.0) (Quinlan, 2014), we extracted those sequences from their respective genomes and used Muscle (v3.8.1551) (Edgar, 2004) to generate pairwise alignments between them and Z32848.1.

Phylogenetic analyses
We downloaded publicly available genome assemblies of *Schizosaccharomyces* species as follows:
S. octosporus - GCA_000150505.2 (Tong et al., 2019)
S. osmophilus - GCA_027921745.1 (Jia et al., 2023)
S. cryophilus - GCA_000004155.2 (Tong et al., 2019)
S. pombe - PomBase (Harris et al., 2022)
S. japonicus (FY16936) - Ensembl Fungi GCA_000149845.2 (Yates et al., 2022)
S. japonicus (FY16936) – EI 1.0 GCA_956476325
Saitoella complicata (outgroup) - GCF_001661265.1 (Nishida, Hamamoto, & Sugiyama, 2011)

For each assembly we ran BUSCO (v5.4.4) using the most up-to-date Ascomycota database (ascomycota_odb10) to identify single-copy orthologs in each assembly. We then took the intersect of orthologs that were found to be complete and in a single copy across all assemblies and created a BED-format file of all those genes across each assembly. Using BEDTools getfasta tools (v2.23.0) (Quinlan, 2014) we extracted the sequence for each ortholog in each species. Next, we created ortholog-specific fasta files for each species and used Muscle to generate multispecies alignments for each ortholog.

We used IQTree2 (v2.2.2.2) (Minh et al., 2020) with default parameters (ModelFinder, tree search, ultrafast bootstrap (1000 replicates) and SH-aLRT test (1000 replicates)) to create a maximum likelihood (ML) phylogeny using all ortholog-specific gene alignments. Then, using Newick utils (v1.5) (Junier & Zdobnov, 2010) we set *S. complicata* as the outgroup. In order to obtain node bootstrap support for the consensus phylogeny, we used IQTree2 to create individual ML phylogenies for each ortholog and then counted the number of times each branch in the original ML tree occurred in the set of ortholog-specific trees, using this rate as the bootstrapping values.

Dating the CBS5679 split from the 'type' strain of S. japonicus
We used seqkit (W. Shen, Le, Li, & Hu, 2016) to concatenate the Muscle alignments for each ortholog. We then used SNP-sites (Page et al., 2016) to extract all variable sites where each nucleotide was either A, T, C, or G. Next, we used RelTree ML and RelTree Branch Lengths in MEGA (Stecher, Tamura, & Kumar, 2020; Tamura et al., 2012; Tamura, Tao, & Kumar, 2018) to date the CBS5679-FY16936 split, using the ortholog SNP-sites alignment data and the ML phylogeny. We used the following previously calculated divergence times (Jia et al., 2023; X. X. Shen et al., 2020):

Split 1. *S. japonicus – S. pombe* split (207.2 million years ago (MYA))
Split 2. *S. pombe – S. octosporus* split (108.2 MYA)

Split 3. *S. octosporus – S. cryophilus* split (29.4 MYA)
Split 4. *S. octosporus – S. osmophilus* split (15.7 MYA)

To compare our calculated divergence time with other previously calculated times, we ran RelTree ML and RelTree Branch Lengths, omitting Split 4 above (*S. octosporus – S. osmophilus*) and compared our predicted divergence time to that of the previously calculated divergence time (Jia et al., 2023).

Genetic crosses
Crosses were performed on Sporulation Agar (SPA) medium (Munz & Leupold, 1970) with the following modifications: 3% agar, and 45 mg/ml each of adenine, histidine, leucine, and uracil. Homothallic and heterothallic strains (see Table 1) were mixed at a 1:10 ratio and incubated for 48 hours at 25°C. Cell mixtures were incubated for 1 hour at 37°C with 0.5% v/v glusulase (Perkin Elmer, NEE154001EA) to digest cell walls of vegetative cells and asci, followed by three washes with 20% ethanol, to ensure that no viable vegetative cells remain. For each cross, 63 random spores were dissected on Yeast Extract with Supplements (YES) agar plates (Petersen & Russell, 2016) using a Singer tetrad dissector (Singer Instruments). Plates were incubated at 30°C for 48 hours, replica plated to YES agar plates containing 75 μg/ml G418 (Sigma-Aldrich, G8168), and incubated at 30°C for a further 24 hours. Plates were scanned using ChemiDoc imager (Bio-Rad) before and after replica plating. The presence or the absence of G418 resistance was confirmed by re-streaking colonies on new G418-containing YES agar plates. Experiments were repeated three times. Statistical analyses were performed in Prism 9 (GraphPad).

Oliferenko Collection No.	Genotype	Notes
SOJ1	*S. japonicus* homothallic	Deposited in ATCC as ATCC10660; in H. Niki collection as NIG2008
SOJ5709	*S. japonicus* (?) homothallic	Deposited in Westerdijk Institute collection as CBS5679
SOJ3657	*S. japonicus gpd1-mNeonGreen:kanMX6* h-	Oliferenko collection; generated in the background of *S. japonicus* h- matsj-P2028 (NIG2028 in H. Niki collection)

Table 1. Strain list, genotypes and collection notes for genetic crosses between different variants of *S. japonicus*.

Identifying structural variants
To identify syntenic chromosomal regions between the CBS5679 and FY16936 assemblies, we used the nucmer tool in the MUMmer toolsuite (Delcher, Salzberg, & Phillippy, 2003) to align contigs of the CBS5679 assembly to the three chromosomes of FY16936, visualising the output in Dot (Nattestad, 2020). In order to further identify synteny, translocations, and rearrangements involving coding genes, we used Support Protocol 2 ('Visualizing syntenies between genomes using BUSCO markers') as set out by (Manni et al., 2021). In order to confirm any large genome rearrangements, we aligned CBS5679 ONT reads >50 kb back to the CBS5679 assembly and visualised those regions using IGV (Thorvaldsdottir, Robinson, & Mesirov, 2013) to check long-read coverage across each region. Additionally, we calculated mean coverage across each rearrangement (including 10kb up and downstream) and compared that to the mean coverage for the whole contig.

GO term enrichment
We inputted the list of 446 genes located in the major translocated region into g:Profiler (Raudvere et al., 2019) and searched all known genes using the reference organism as '*S. japonicus*', using the default significance threshold of p>0.05. g:Profiler is a web-based collection of tools that performs functional enrichment analyses of Ensembl gene lists. It maps the gene lists to known functional information sources and detects statistically significantly enriched biological processes and pathways. It is one of the few GO term enrichment tool that allows direct analysis of Ensembl Fungi genes.

Assembly of a scaffolded chromosome-scale assembly
Using information gleaned from the previous analyses, we assembled a chromosome-scale assembly by using alignment information and ortholog placements, and orienting and joining contigs from CBS5679 relative to the FY16936 assembly and gap-filling with N's. For the mitochondrial genome, we completed a self-vs-self blast search and trimmed redundancy from overlapping ends.

Results
Genome assembly and quality control
After assembling with Canu and carrying out three rounds of Pilon polishing, our assembly consisted of 46 contigs, totalling 16,207,024 bps. We compared the number of single-copy orthologs resolved in the assembly to those in the Ensembl Fungi *S. japonicus* assembly (GCA_000149845.2) and found that the number of single-copy, fragmented, duplicated, and missing orthologs only varied by a maximum of 0.3% (Figure 1). Additionally, we compared repeat content of CBS5679 to that of a telomere-to-telomere genome assembly of *S. japonicus* (FY16936; referred to as *S. japonicus* EI 1.0 assembly; GCA_956476325). We found that CBS5679 had 4% more repeat content than the *S. japonicus* EI 1.0 assembly and, like that assembly, most identified repeats belonged to the LTRs and Helitron-like transposons (Table 2). Genome annotation files for coding sequences, rRNA genes, tRNA genes, and repeats can be found in the Supplementary Data (Supplementary data S1).

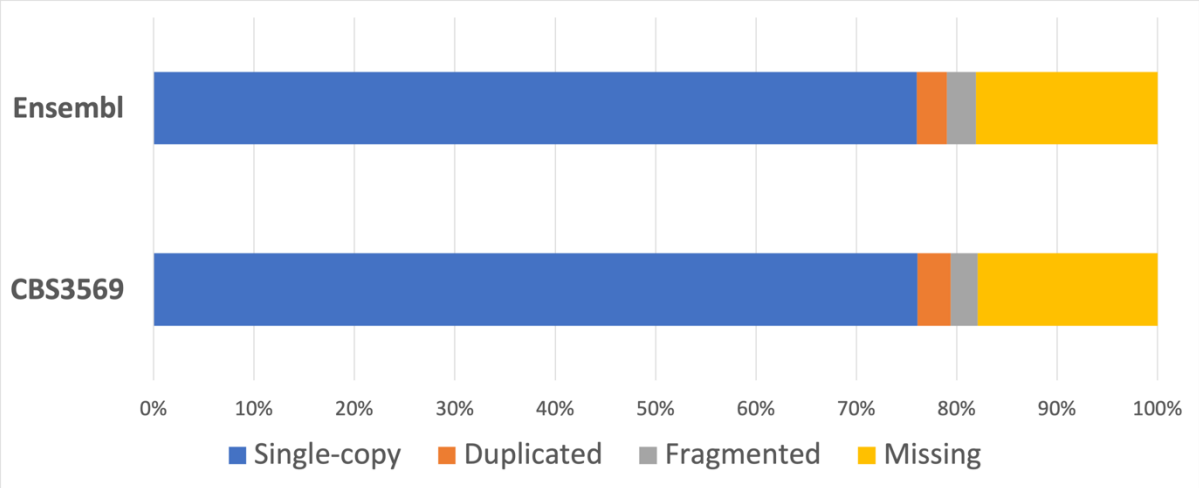

Figure 1. Comparison of BUSCO single-copy ortholog resolution between CBS3569 and Ensembl Fungi S. *japonicus*.

Repeat class	CBS5679	EI 1.0
Nucleotides masked	3,033,726	2,472,691
% SINE	0.004	0.10
% LTR	12.58	11.56
% RC (Helitron)	1.02	2.02
% Unknown	4.32	1.21
% masked	18.7	14.89

Table 2. Comparison of assembly repeat content (%) by class between CBS5679 and FY16936 (EI 1.0). Abbreviations: SINE - Short interspersed nuclear elements; LTR - long terminal repeat; RC – rolling circle transposons (Helitron-like transposons).

We compared the percentage nucleotide identity between Nanopore reads of FY16936 and CBS5679 to that of the CDS sequences of *S. japonicus* in Ensembl Fungi. We found that FY16936 reads showed a 99.96% identity to *S. japonicus* CDS sequences and CBS5679 showed only 88.44% identity (Table 3). This difference in identity could not be explained by Nanopore sequencing error rates (which would be equivalent for both datasets) or differences in mean alignment lengths (which are also similar). The number of mismatches and gaps opened in CBS5679 were 180 and 62 times greater (respectively) than in FY16936.

Dataset	% identity	Mean alignment length	Mean No. mismatches	Mean No. gaps opened
FY16936 reads	99.96	1693	0.098	0.25
CBS5679 reads	88.44	1641	176.036	15.39

Table 3. Comparison of ONT read alignments for *S. japonicus* FY16936 and CBS5679 against CDS sequences for the Ensembl Fungi *S. japonicus* assembly.

Comparison to S. japonicus var. versatilis rRNA

We compared 6.5 kb of previously reported sequence from the 17S, 5.8S, and 25S rRNA genes (including ITS1 and ITS2) from *S. japonicus* var. *versatilis* (Z32848.1) to that of CBS5679 and FY16936 (Table 4). We did not identify any differences within ITS1 or 5.8S. Across all features, *S. japonicus* var. *versatilis* and CBS5679 were the most similar (25 SNPs), followed by CBS5679 and *S. japonicus* EI 1.0 (48 SNPs). Finally, *S. japonicus* var. *versatilis* and *S. japonicus* EI 1.0 showed the greatest distance (73 SNPs).

Feature	length	*S. japonicus* var. *versatilis* vs CBS5679	*S. japonicus* var. *versatilis* vs EI 1.0	CBS5679 vs EI 1.0
17S	2019	0.00149 (3)	0.00198 (4)	0.00050 (1)
ITS1	186	0	0	0
5.8S	157	0	0	0
ITS2	268	0	0.08582 (23)	0.08582 (23)
25S	3433	0.00641 (22)	0.01340 (46)	0.00699 (24)
Total	6063	0.00412 (25)	0.01204 (73)	0.00792 (48)

Table 4. Pairwise comparisons of 17S, 5.8S, and 25S ribosomal RNA genes, including Internal Transcribed Spacer (ITS) 1 and ITS2 between *S. japonicus* var. *versatilis,* CBS5679, and *S. japonicus* EI 1.0. Values represent divergence, calculated by the number of SNPs divided by the length of the feature. Numbers in brackets are the absolute number of SNPS.

Phylogenetic analysis of CBS5679

We ran BUSCO on CBS5679 along with six other *Schizosaccharomyces* assemblies plus one Taphrinomycotina outgroup (*Saitoella complicata*) and resolved 1023 single-copy orthologs present in all assemblies. After creating ortholog-specific alignments, we generated a ML tree using all alignments. The best-fit model of GTR+F+I+R2 was chosen according to the Bayesian information criterion (BIC). We then created ML trees for each of the 1023 orthologs and used those trees to provide bootstrapping support for the original ML tree (Figure 2). CBS5679 splits from both *S. japonicus* assemblies with 99% bootstrap support, providing high confidence for the split.

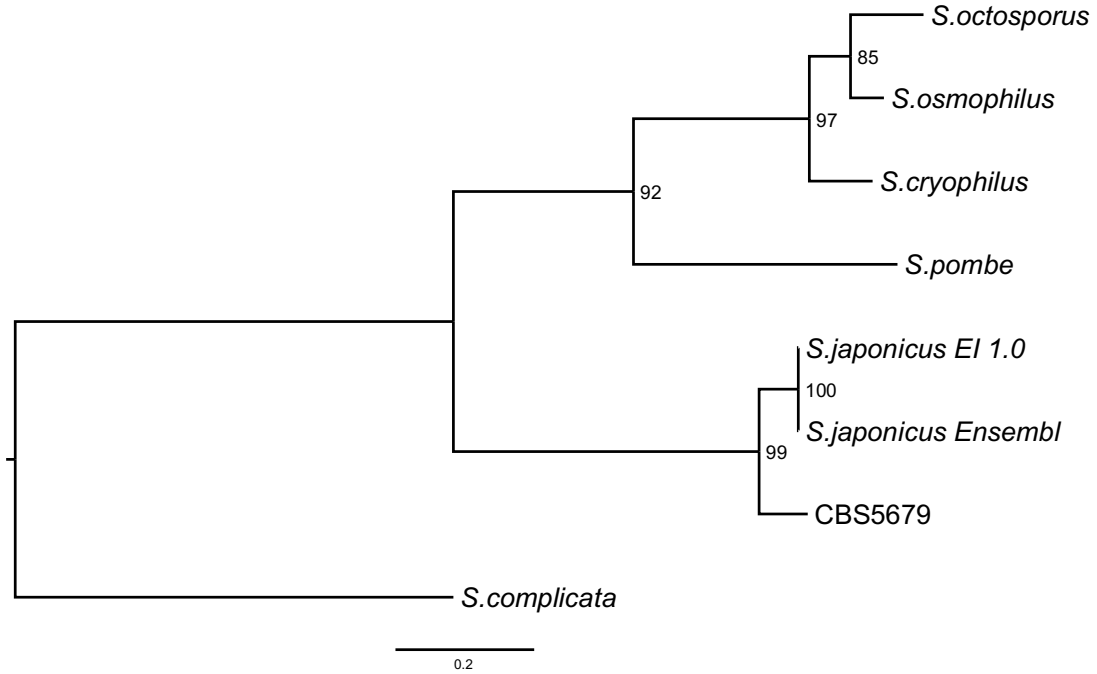

Figure 2. Maximum likelihood (ML) tree based on 1023 single-copy orthologs. Node labels represent bootstrap values from individual ML ortholog trees.

CBS5679 has split from S. japonicus approximately 25 million years ago

Using the ML tree generated above along with 968,591 variable sites contained within the 1023 concatenated, aligned single-copy orthologs, and previously calculated divergence times, we calculated the divergence time of *S. japonicus* and CBS5679. Using RelTree ML, the split was dated at 25.05 MYA (Figure 3) and using RelTree branch length, 24.69 MYA. Additionally, we removed the previously calculated split between *S. octosporus* and *S. osmophilus* from the tree to confirm that this dating-method recapitulated the previously calculated divergence time (Jia et al., 2023). RelTree ML and RelTree branch lengths dated this split at 16.27 MYA and 16.02 MYA respectively (and confirmed the *S. japonicus* and CBS5679 divergence time), closely reflecting the previously calculated divergence time of 15.7 MYA (Jia et al., 2023) (Supplementary Figure S1).

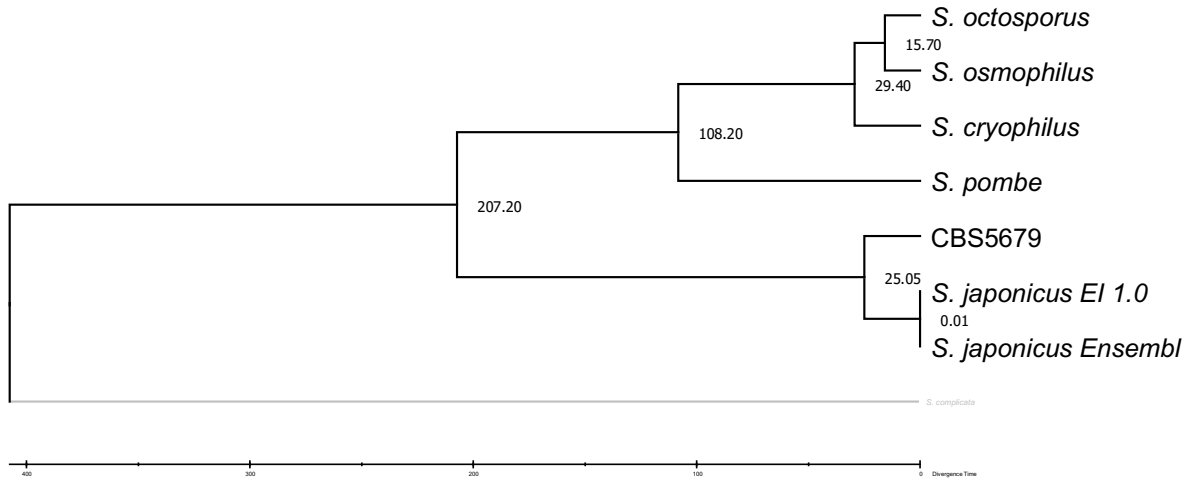

Figure 3. Dated divergence of CBS5679 from *S. japonicus* using RelTree ML. The node numbers represent divergence times in millions of years.

CBS5679 does not generate viable progeny in crosses with the type S. japonicus strain
To test if the CBS5679 strain (Bouwknegt et al., 2021) could generate viable progeny with *S. japonicus*, we performed crosses between the homothallic CBS5679, or the "type" homothallic *S. japonicus* isolate (ATCC10660) and a heterothallic h- strain of *S. japonicus* (Furuya & Niki, 2009), where the glycerol-3-phosphate dehydrogenase Gpd1 was marked with the G418-resistance cassette (Ying Gu, Alam, & Oliferenko, 2023) .We used the heterothallic h- strain in excess (see Materials and Methods for details), since both homothallic strains sporulate with high efficiency. As controls, we included either CBS5679 or ATCC10660 sporulating individually.

Following sporulation, we dissected and plated individual spores to ensure that no vegetative cells contribute to our analyses. Spores originating from crosses containing the CBS5679 strain germinated and formed colonies at higher frequency as compared to those containing the "type" ATCC10660 *S. japonicus* isolate (Figure 4A). The introduction of the heterothallic h- strain into crosses with either homothallic strain did not affect overall spore germination and colony formation efficiency (Figure 4A). Of note, we observed the appearance of G418-resistance only in the crosses between ATCC10660 and the G418-resistance-marked h- *S. japonicus* strain (Figure 4B). In our experimental conditions, the proportion of G418-resistant colonies was consistent between three different experiments and averaged ~34%. We concluded that it was likely that CBS5679 strain has become reproductively isolated from the "type" strain of *S. japonicus*.

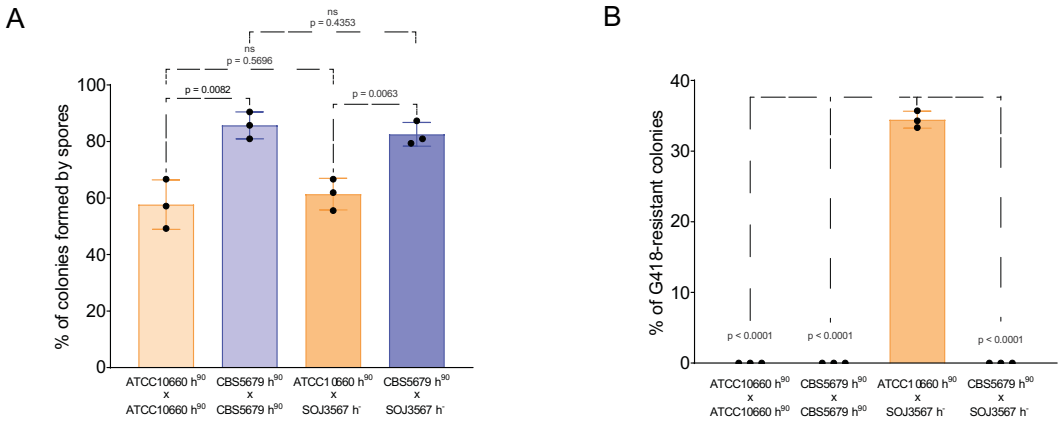

Figure 4. (A) Graph illustrating the efficiency of colony formation by spores formed in crosses of indicated genotypes. (B) Graph showing the percentage of G418-resistant colonies in crosses of indicated genotypes. (A-B) Experiments were performed in three biological replicates and *p-values* were derived using unpaired parametric t test.

The genomes of CBS5679 and the type S. japonicus strain exhibit major structural variation
Using Nucmer, we aligned the contigs from CBS5679 to that of the three chromosomes of *S. japonicus* EI 1.0 to identify syntenic regions, translocations, and inversions (Figure 5). Additionally, we plotted the BUSCO single-copy orthologs present on both genomes to identify the genomic locations of orthologs between the two assemblies (Figure 6).

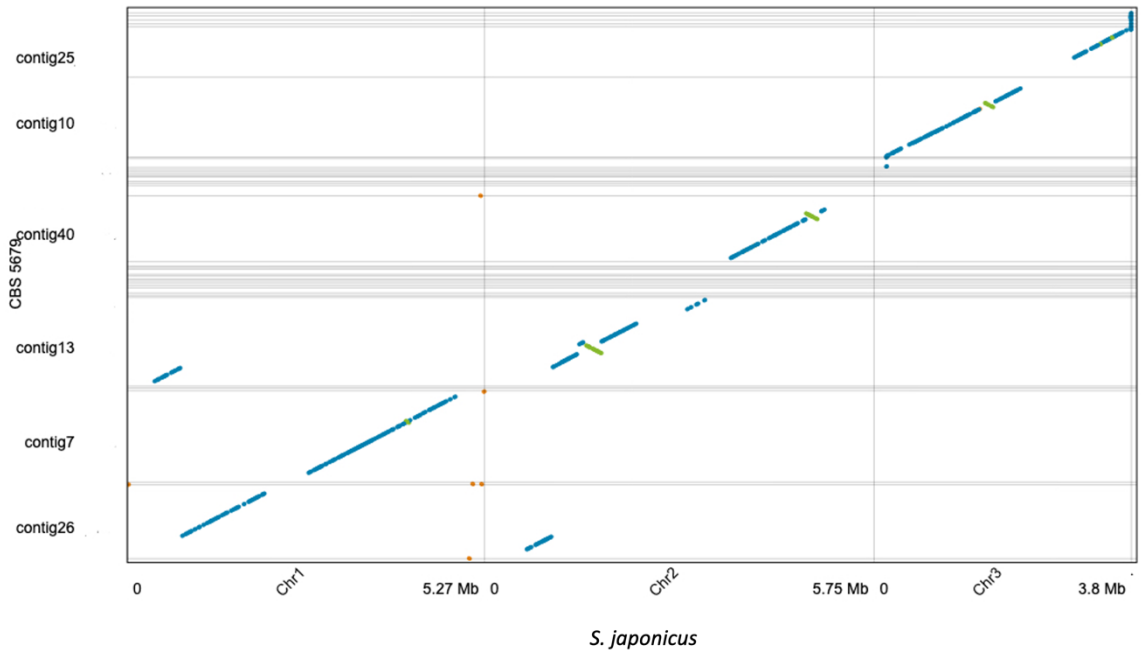

Figure 5. Alignment of CBS5679 to *S. japonicus* EI 1.0 showing syntenic regions and translocation involving Chr1 and Chr2. Blue lines refer to forward alignments and green lines refer to reverse alignments (inversions). Reciprocal translocations can be seen between *S. japonicus* 'Chr1' and 'Chr2' and CBS5679 'contig13' and 'contig26'.

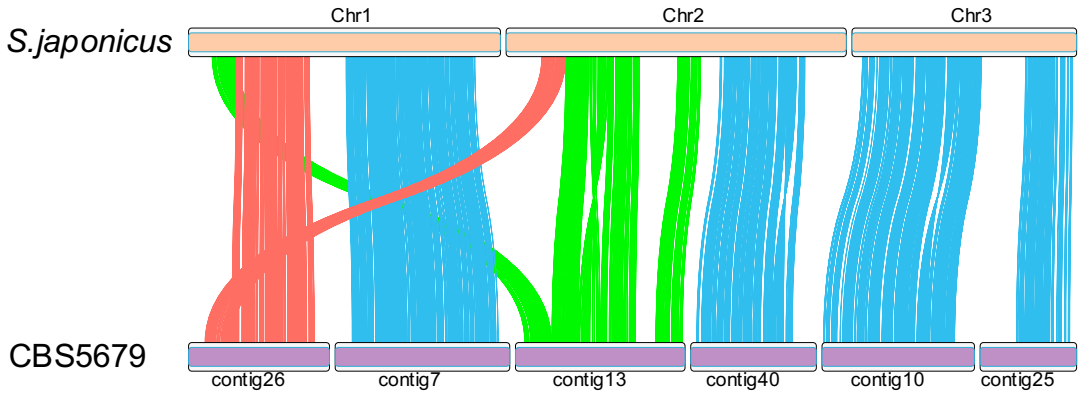

Figure 6. Placement of BUSCO single-copy orthologs present on both *S. japonicus* EI 1.0 and CBS5679. Orthologs present on CBS5679 contig13 are mapped in green and those on contig26 are mapped in red, showing the location of orthologs involved in a reciprocal translocation.

It is clear there is a reciprocal translocation involving chromosomes 1 and 2 in *S. japonicus*, and contig26 and contig13 on CBS5679. Using the mapping locations of the orthologs (Supplementary Table S1), we identified the approximate location of the translocations, which occurred between position 799,696 and 808,427 on Chr 1 and positions 1,004,860 and 1,010,039 on Chr 2 (Table 5).

	S. japonicus EI 1.0			CBS5679		
Ortholog name	Chromosome	Ortholog start	Ortholog end	Contig	Ortholog start	Ortholog end
85315at4890	1	797053	799696	contig13	536839	539492
213148at4890	1	808427	810400	contig26	1457191	1459164
338471at4890	2	1004387	1004860	contig26	1464423	1464842
202577at4890	2	1010039	1011033	contig13	547711	548705

Table 5. The approximate sites of the translocation between *S. japonicus* Chr 1 and Chr2 and CBS5679 contig13 and contig26. The ortholog name is that from BUSCO odb10 and the co-ordinates refer to each given ortholog in each assembly.

We aligned CBS5679 ONT reads >50kb back to the CBS5679 assembly and visualised the regions on contig13 and contig26, which contained the translocations (Supplementary Figure S2). In both cases it was clear that no misassemblies had taken place with long reads spanning both regions. Additionally, mean long-read coverage across each translocated region of CBS5679 was close to the mean for the whole contig. Specifically, the mean coverage for contig26 was 10 (SD 3.25) and the mean coverage over the translocation was 10 (SD 0.66). The mean coverage for contig13 was 9 (SD 4.23) and the mean coverage over the translocation was 7 (SD 1.42).

In addition, three large inversions can be seen between the two assemblies (denoted by the green lines in Figure 5, and large 'twists' in the ortholog mapping in Figure 6). The length of the large inversions varied between 147.2 kb and 307 kb (Table 6).

EI 1.0 chromosome	start	end	size	CB5679 contig
2	1416577	1723660	307,084	contig13
2	4763199	4960096	196,898	contig40
3	1615898	1763107	147,210	contig10

Table 6. Location and size of inversions between CBS5679 and *S. japonicus* EI 1.0. Locations are given relative to EI 1.0. CBS5679 contig refers to the contig containing the inversion.

Major chromosomal rearrangement carries genes associated with metabolism and cellular organization

Large genomic rearrangements are often responsible for pre-zygotic barriers between interspecies hybridisation. We identified genes on translocated genomic loci and carried out Gene Ontology (GO) term enrichment analyses. Given a list of genes from an experiment, GO term enrichment identifies the pathways each gene is involved in and then identifies pathways that have more genes than expected by chance. We identified 446 protein-coding genes situated in chromosomes 1 and 2 that lay within the reciprocal translocation with CBS5679 and analysed them for enriched GO terms (Table 7). Although many of the significant terms were high-level (e.g., 'molecular_function', 'biological_process', 'cellular_process', etc.), many other terms fell into one of two different terms: "metabolic processing", and "cellular assembly". Metabolic processing terms include homoserine metabolic process, primary metabolic process, organic substance metabolic process, and metabolic process, whilst cellular assembly terms include cellular component assembly, cellular component biogenesis, cellular anatomical entity, cellular component, actin cortical patch, endocytic patch, and cortical actin cytoskeleton.

GO category	Term name	GO term ID	Adjusted p-value
GO:MF	molecular_function	GO:0003674	7.61E-08
GO:BP	biological_process	GO:0008150	1.48125E-05
GO:BP	cellular process	GO:0009987	0.000756756
GO:BP	cellular component assembly	GO:0022607	0.001871718
GO:BP	primary metabolic process	GO:0044238	0.002338023
GO:BP	homoserine metabolic process	GO:0009092	0.012502301
GO:BP	cellular component biogenesis	GO:0044085	0.017597583
GO:BP	organic substance metabolic process	GO:0071704	0.024054927
GO:BP	metabolic process	GO:0008152	0.030869142
GO:CC	cellular anatomical entity	GO:0110165	2.56903E-06
GO:CC	cellular_component	GO:0005575	9.65011E-06
GO:CC	actin cortical patch	GO:0030479	0.017274955
GO:CC	endocytic patch	GO:0061645	0.022400654

GO:CC	cortical actin cytoskeleton	GO:0030864	0.046312161

Table 7. Enriched gene ontology (GO) terms identified from 446 protein-coding genes located within the reciprocal translocation. The GO categories are as follows: GO:MF – molecular function, GO:BP – biological process, GO:CC – cellular component. The full analyses, including all input data, run parameters and options may be found at the following URL: https://biit.cs.ut.ee/gplink/l/DclCMvGJSh

Assembly of a scaffolded chromosome-scale assembly

Our final assembly, (ACCESSION NUMBER HERE), comprised of three autosomal chromosomes, one mitochondrial genome, plus 39 unplaced contigs. The combined total of the three autosomal chromosomes plus mitochondrial genome was 13.3Mb (including Ns) and 16.5 Mb including the unplaced contigs.

Discussion

We have assembled and annotated the genome of CBS5679 that was originally assumed to be a strain of *Schizosaccharomyces japonicus* var. *versatilis*. The unscaffolded assembly is 16.2 Mb of which 12.9 Mb is represented by 6 contigs that each align to a chromosome arm of the reference strain of *S. japonicus*. The number of single-copy orthologs is almost identical to that of the Ensembl Fungi reference of *S. japonicus* and the percentage of the genome masked is similar, although the number of repeats of 'Unknown' class was greater in CBS5679. Yet, at the CDS level CBS5679 significantly diverges from S. *japonicus*, sharing only 88.4% sequenced identity. Phylogenetically CBS5679 is a separate sister clade to *S. japonicus* (supported by 99% bootstrap values). The timing of this split is estimated to be around 25.05 MYA, and the accuracy of this estimate is further supported by our estimate of the *S. octosporus* - *S. osmophilus* split, which was within 0.3 MY of the previously calculated split (Jia et al., 2023).

Over the 17S, 5.8S and 25S rRNA unit, CBS5679 shows much greater similarity to *S. japonicus* var. *versatilis*, showing approximately half as many differences to that strain than FY16936 (var. *japonicus*) and possibly reflects the genetic variation found within *S. versatilis*, or perhaps represents population structure within the species.

When compared to *S. japonicus* FY16936, CBS5679 has a reciprocal translocation between chromosomes 1 and 2, with roughly 800 kb from chromosome 1 on FY16936 now being located on CBS5679 chromosome 2, and 1 Mb of chromosome 2 on FY16936 now being located on CBS5679 chromosome 1. Additionally, CBS5679 contains at least three large scale (> 140 kb) inversions. In *Saccharomyces cerevisiae* it was found that if two genes were closely located, they were more likely to be involved in the same biological process (Santoni, Castiglione, & Paci, 2013). The largest metabolic gene cluster in yeast (the DAL cluster), was assembled through an almost simultaneous set of telomeric rearrangements that brought together the genes in this pathway (Wong & Wolfe, 2005). Furthermore, work on *S. pombe* showed that chromosomal rearrangements contribute to reproductive success and could be strongly beneficial in one environment but deleterious in another. These rearrangements were also accompanied by alterations in gene expression (Teresa Avelar, Perfeito, Gordo, & Godinho Ferreira, 2013). These large chromosomal rearrangements reported here could be one of the reasons for reproductive isolation between CBS5679 and the 'type' strain of *S. japonicus*.

Experimentally, we demonstrate that CBS5679 is reproductively isolated from the *S. japonicus* 'type' strain. A heterothallic h- strain of *S. japonicus*, marked with an G418-resistance gene, efficiently generated G418 resistant spores when crossed with a homothallic *S. japonicus* isolate, but not with the homothallic CBS5679 isolate. This cannot be explained by a failure in sporulation or germination for the CBS5679 isolate, since both processes were equivalent or occurred more efficiently in CBS5679 than in the *S. japonicus* 'type' strain.

Interestingly, GO enriched terms for genes located in the translocated regions fell mainly into two categories: metabolic processing, and cellular assembly. CBS5679 and other *S. versatilis* strains share a number of metabolic characteristics with the type strain of *S. japonicus*, including anaerobic growth and the inability to utilize non-fermentable carbon sources (Alam, Gu, Reichert, Bahler, & Oliferenko, 2023; Bouwknegt et al., 2021; Bulder, 1963, 1971; Wickerham & Duprat, 1945). Yet, some aspects of amino acid biosynthesis and energy and redox metabolism might have been rewired after the split between the two species. For instance, it would be of interest to revisit the older biochemical data on the differences in the complement of cellular cytochromes between *S. japonicus* and *S. versatilis* in light of the newly available genomes and our current understanding of fission yeast metabolism and physiology (Alam et al., 2023; Ying Gu et al., 2023; Kaino, Tonoko, Mochizuki, Takashima, & Kawamukai, 2018).

Within the cellular assembly category, cortical actin and endocytic patch terms are significantly enriched. Cortical actin filaments nucleated by formins mediate long-range vesicle trafficking, which is required for the polarized growth of vegetative cells and the formation of specialized fusion structures essential for mating. A different type of actin networks, the Arp2/3-nucleated "patches" promote the formation and movement of endocytic vesicles, enabling nutrient uptake and polarized growth. During cell division, actin-based structures ensure cortical ingression and eventual separation of the daughter cells (Kovar, Sirotkin, & Lord, 2011; Mishra, Huang, & Balasubramanian, 2014). Together with metabolism, actin cytoskeleton impinges on virtually every aspect of biology. Understanding the phylogenetic relationship between *S. japonicus* and *S. versatilis* and the availability of high-quality genome assemblies for both species will undoubtedly facilitate mechanistic evolutionary cell biology studies using fission yeasts.

We conclude that CBS5679, a representative of *S. japonicus* var. *versatilis*, is a phylogenetically distinct species. Having diverged around 25 MYA, it is only 88% identical at the CDS level to *S. japonicus*, its genome contains large-scale translocations and inversions, and it does not readily cross with *S. japonicus* var. *japonicus*. We recommend that the taxonomic status of *S. japonicus* var. *versatilis* is raised and that it should be treated as a separate species within the fission yeast clade, *Schizosaccharomyces versatilis*.

Acknowledgements
We acknowledge Frank Uhlmann for reading and commenting on this manuscript. We thank Li-Lin Du and Guo-Song Jia for helpful comments and sharing unpublished results.
GJE assembled and annotated the assembly and carried out all bioinformatic and phylogenetic analyses. EGG and SO carried out the genetic crosses. CN, SO, and WH assisted with experimental design. All authors contributed to writing and reviewing the manuscript.

Data availability

The genome assembly for *S. versatilis* can be found under ENA Project PRJEB63472, with an accession number of CATQFW010000000.

Conflict of interest statement
The authors declare no conflict of interest.

Funding
G.J.E., W.H., and C.A.N. acknowledge funding from the from the Biotechnology and Biological Sciences Research Council (BBSRC), part of UK Research and Innovation, Core Capability Grant BB/CCG1720/1. This research was supported in part by the NBI Research Computing through use of the High-Performance Computing system and Isilon storage. E.G.G is funded through a long-term EMBO postdoctoral fellowship (ALTF 712-2022). Work in S.O. lab is supported by the Wellcome Trust Investigator Award in Science (220790/Z/20/Z) and BBSRC (BB/T000481/1) to Snezhana Oliferenko.

References:

Alam, S., Gu, Y., Reichert, P., Bahler, J., & Oliferenko, S. (2023). Optimization of energy production and central carbon metabolism in a non-respiring eukaryote. *Curr Biol, 33*(11), 2175-2186 e2175. doi:10.1016/j.cub.2023.04.046

Aoki, K., Hayashi, H., Furuya, K., Sato, M., Takagi, T., Osumi, M., . . . Niki, H. (2011). Breakage of the nuclear envelope by an extending mitotic nucleus occurs during anaphase in Schizosaccharomyces japonicus. *Genes Cells, 16*(9), 911-926. doi:10.1111/j.1365-2443.2011.01540.x

Belser, C., Baurens, F. C., Noel, B., Martin, G., Cruaud, C., Istace, B., . . . Aury, J. M. (2021). Telomere-to-telomere gapless chromosomes of banana using nanopore sequencing. *Commun Biol, 4*(1), 1047. doi:10.1038/s42003-021-02559-3

Bouwknegt, J., Wiersma, S. J., Ortiz-Merino, R. A., Doornenbal, E. S. R., Buitenhuis, P., Giera, M., . . . Pronk, J. T. (2021). A squalene-hopene cyclase in Schizosaccharomyces japonicus represents a eukaryotic adaptation to sterol-limited anaerobic environments. *Proc Natl Acad Sci U S A, 118*(32). doi:10.1073/pnas.2105225118

Brysch-Herzberg, M., Jia, G.-S., Seidel, M., Assali, I., & Du, L.-L. (2022). Insights into the ecology of Schizosaccharomyces species in natural and artificial habitats. *Antonie van Leeuwenhoek, 115*(5), 661-695.

Brysch-Herzberg, M., Jia, G. S., Sipiczki, M., Seidel, M., Li, W., Assali, I., & Du, L. L. (2023). Schizosaccharomyces lindneri sp. nov., a fission yeast occurring in honey. *Yeast*. doi:10.1002/yea.3857

Bulder, C. J. (1963). *On respiratory deficiency in yeasts.* (PhD). TU Delft, Retrieved from http://resolver.tudelft.nl/uuid:4017a4eb-606c-4669-a1a3-d91df94bc51e

Bulder, C. J. (1971). Anaerobic growth, ergosterol content and sensitivity to a polyene antibiotic, of the yeast Schizosaccharomyces japonicus. *Antonie van Leeuwenhoek, 37*(3), 353-358. doi:10.1007/BF02218505

Chan, P. P., Lin, B. Y., Mak, A. J., & Lowe, T. M. (2021). tRNAscan-SE 2.0: improved detection and functional classification of transfer RNA genes. *Nucleic Acids Res, 49*(16), 9077-9096. doi:10.1093/nar/gkab688

Chapman, E., Taglini, F., & Bayne, E. H. (2022). Separable roles for RNAi in regulation of transposable elements and viability in the fission yeast Schizosaccharomyces japonicus. *PLoS Genet, 18*(2), e1010100. doi:10.1371/journal.pgen.1010100

Delcher, A. L., Salzberg, S. L., & Phillippy, A. M. (2003). Using MUMmer to identify similar regions in large sequence sets. *Curr Protoc Bioinformatics, Chapter 10*, Unit 10 13. doi:10.1002/0471250953.bi1003s00

Edgar, R. C. (2004). MUSCLE: multiple sequence alignment with high accuracy and high throughput. *Nucleic Acids Res, 32*(5), 1792-1797. doi:10.1093/nar/gkh340

Flynn, J. M., Hubley, R., Goubert, C., Rosen, J., Clark, A. G., Feschotte, C., & Smit, A. F. (2020). RepeatModeler2 for automated genomic discovery of transposable element families. *Proc Natl Acad Sci U S A, 117*(17), 9451-9457. doi:10.1073/pnas.1921046117

Furuya, K., & Niki, H. (2009). Isolation of heterothallic haploid and auxotrophic mutants of Schizosaccharomyces japonicus. *Yeast, 26*(4), 221-233. doi:10.1002/yea.1662

Furuya, K., & Niki, H. (2010). The DNA damage checkpoint regulates a transition between yeast and hyphal growth in Schizosaccharomyces japonicus. *Mol Cell Biol, 30*(12), 2909-2917. doi:10.1128/MCB.00049-10

Furuya, K., & Niki, H. (2012). Hyphal differentiation induced via a DNA damage checkpoint-dependent pathway engaged in crosstalk with nutrient stress signaling in Schizosaccharomyces japonicus. *Curr Genet, 58*(5-6), 291-303. doi:10.1007/s00294-012-0384-4

Gomez-Gil, E., Franco, A., Madrid, M., Vazquez-Marin, B., Gacto, M., Fernandez-Breis, J., . . . Cansado, J. (2019). Quorum sensing and stress-activated MAPK signaling repress yeast to hypha transition in the fission yeast Schizosaccharomyces japonicus. *PLoS Genet, 15*(5), e1008192. doi:10.1371/journal.pgen.1008192

Gu, Y., Alam, S., & Oliferenko, S. (2023). Peroxisomal compartmentalization of amino acid biosynthesis reactions imposes an upper limit on compartment size. *bioRxiv*, 2023.2003. 2006.531353.

Gu, Y., & Oliferenko, S. (2019). Cellular geometry scaling ensures robust division site positioning. *Nat Commun, 10*(1), 268. doi:10.1038/s41467-018-08218-2

Gu, Y., Yam, C., & Oliferenko, S. (2015). Rewiring of cellular division site selection in evolution of fission yeasts. *Curr Biol, 25*(9), 1187-1194. doi:10.1016/j.cub.2015.02.056

Harris, M. A., Rutherford, K. M., Hayles, J., Lock, A., Bahler, J., Oliver, S. G., . . . Wood, V. (2022). Fission stories: using PomBase to understand Schizosaccharomyces pombe biology. *Genetics, 220*(4). doi:10.1093/genetics/iyab222

Jia, G. S., Zhang, W. C., Liang, Y., Liu, X. H., Rhind, N., Pidoux, A., . . . Du, L. L. (2023). A high-quality reference genome for the fission yeast Schizosaccharomyces osmophilus. *G3 (Bethesda)*. doi:10.1093/g3journal/jkad028

Johannsen, E. (1981). Hybridization studies within the genus Schizosaccharomyces Lindner. *Canadian Journal of Microbiology, 27*(2), 184-191.

Junier, T., & Zdobnov, E. M. (2010). The Newick utilities: high-throughput phylogenetic tree processing in the UNIX shell. *Bioinformatics, 26*(13), 1669-1670. doi:10.1093/bioinformatics/btq243

Kaino, T., Tonoko, K., Mochizuki, S., Takashima, Y., & Kawamukai, M. (2018). Schizosaccharomyces japonicus has low levels of CoQ(10) synthesis, respiration deficiency, and efficient ethanol production. *Biosci Biotechnol Biochem, 82*(6), 1031-1042. doi:10.1080/09168451.2017.1401914

Kinnaer, C., Dudin, O., & Martin, S. G. (2019). Yeast-to-hypha transition of Schizosaccharomyces japonicus in response to environmental stimuli. *Molecular Biology of the Cell, 30*(8), 975-991. doi:10.1091/mbc.E18-12-0774

Klar, A. J. (2013). Schizosaccharomyces japonicus yeast poised to become a favorite experimental organism for eukaryotic research. *G3 (Bethesda), 3*(10), 1869-1873. doi:10.1534/g3.113.007187

Koren, S., Walenz, B. P., Berlin, K., Miller, J. R., Bergman, N. H., & Phillippy, A. M. (2017). Canu: scalable and accurate long-read assembly via adaptive k-mer weighting and repeat separation. *Genome Res, 27*(5), 722-736. doi:10.1101/gr.215087.116

Kovar, D. R., Sirotkin, V., & Lord, M. (2011). Three's company: the fission yeast actin cytoskeleton. *Trends Cell Biol, 21*(3), 177-187. doi:10.1016/j.tcb.2010.11.001

Kurtzman, C. P., & Sugiyama, J. (2015). 1 Saccharomycotina and Taphrinomycotina: The yeasts and yeastlike Fungi of the Ascomycota. *Systematics and evolution: Part B*, 3-33.

Lee, I. J., Stokasimov, E., Dempsey, N., Varberg, J. M., Jacob, E., Jaspersen, S. L., & Pellman, D. (2020). Factors promoting nuclear envelope assembly independent of the canonical ESCRT pathway. *J Cell Biol, 219*(6). doi:10.1083/jcb.201908232

Liu, Y., Leigh, J. W., Brinkmann, H., Cushion, M. T., Rodriguez-Ezpeleta, N., Philippe, H., & Lang, B. F. (2009). Phylogenomic analyses support the monophyly of Taphrinomycotina, including Schizosaccharomyces fission yeasts. *Mol Biol Evol, 26*(1), 27-34. doi:10.1093/molbev/msn221

Makarova, M., Gu, Y., Chen, J. S., Beckley, J. R., Gould, K. L., & Oliferenko, S. (2016). Temporal Regulation of Lipin Activity Diverged to Account for Differences in Mitotic Programs. *Curr Biol, 26*(2), 237-243. doi:10.1016/j.cub.2015.11.061

Makarova, M., Peter, M., Balogh, G., Glatz, A., MacRae, J. I., Lopez Mora, N., . . . Oliferenko, S. (2020). Delineating the Rules for Structural Adaptation of Membrane-Associated Proteins to Evolutionary Changes in Membrane Lipidome. *Curr Biol, 30*(3), 367-380 e368. doi:10.1016/j.cub.2019.11.043

Manni, M., Berkeley, M. R., Seppey, M., & Zdobnov, E. M. (2021). BUSCO: Assessing Genomic Data Quality and Beyond. *Curr Protoc, 1*(12), e323. doi:10.1002/cpz1.323

Martini, A. V. (1991). Evaluation of phylogenetic relationships among fission yeast by nDNA/nDNA reassociation and conventional taxonomic criteria. *Yeast, 7*(1), 73-78.

Minh, B. Q., Schmidt, H. A., Chernomor, O., Schrempf, D., Woodhams, M. D., von Haeseler, A., & Lanfear, R. (2020). IQ-TREE 2: New Models and Efficient Methods for Phylogenetic Inference in the Genomic Era. *Mol Biol Evol, 37*(5), 1530-1534. doi:10.1093/molbev/msaa015

Mishra, M., Huang, J., & Balasubramanian, M. K. (2014). The yeast actin cytoskeleton. *FEMS Microbiol Rev, 38*(2), 213-227. doi:10.1111/1574-6976.12064

Munz, P., & Leupold, U. (1970). Characterization of ICR-170-induced mutations in Schizosaccharomyces pombe. *Mutat Res, 9*(2), 199-212. doi:10.1016/0027-5107(70)90058-8

Naehring, J., Kiefer, S., & Wolf, K. (1995). Nucleotide sequence of the Schizosaccharomyces japonicus var. versatilis ribosomal RNA gene cluster and its phylogenetic implications. *Curr Genet, 28*(4), 353-359. doi:10.1007/BF00326433

Nattestad, M. (2020). Dot (Version b18fed0). Retrieved from https://github.com/MariaNattestad/dot

Nishida, H., Hamamoto, M., & Sugiyama, J. (2011). Draft genome sequencing of the enigmatic yeast Saitoella complicata. *The Journal of general and applied microbiology, 57*(4), 243-246.

Nozaki, S., Furuya, K., & Niki, H. (2018). The Ras1-Cdc42 pathway is involved in hyphal development of Schizosaccharomyces japonicus. *FEMS Yeast Res, 18*(4). doi:10.1093/femsyr/foy031

Nurk, S., Koren, S., Rhie, A., Rautiainen, M., Bzikadze, A. V., Mikheenko, A., . . . Phillippy, A. M. (2022). The complete sequence of a human genome. *Science, 376*(6588), 44-53. doi:10.1126/science.abj6987

Page, A. J., Taylor, B., Delaney, A. J., Soares, J., Seemann, T., Keane, J. A., & Harris, S. R. (2016). SNP-sites: rapid efficient extraction of SNPs from multi-FASTA alignments. *Microb Genom, 2*(4), e000056. doi:10.1099/mgen.0.000056

Papp, L. A., Acs-Szabo, L., Batta, G., & Miklos, I. (2021). Molecular and comparative genomic analyses reveal evolutionarily conserved and unique features of the Schizosaccharomyces japonicus mycelial growth and the underlying genomic changes. *Curr Genet, 67*(6), 953-968. doi:10.1007/s00294-021-01206-y

Petersen, J., & Russell, P. (2016). Growth and the Environment of Schizosaccharomyces pombe. *Cold Spring Harb Protoc, 2016*(3), pdb top079764. doi:10.1101/pdb.top079764

Phaff, H., Yoneyama, M., & CARMO-SOUSA, L. D. (1964). A one-year, quantitative study of the yeast flora in a single slime flux of Ulmus carpinifolia Gled. *Rivista di Patologia Vegetale*, 485-497.

Pieper, G. H., Sprenger, S., Teis, D., & Oliferenko, S. (2020). ESCRT-III/Vps4 Controls Heterochromatin-Nuclear Envelope Attachments. *Dev Cell, 53*(1), 27-41 e26. doi:10.1016/j.devcel.2020.01.028

Quinlan, A. R. (2014). BEDTools: The Swiss-Army Tool for Genome Feature Analysis. *Curr Protoc Bioinformatics, 47*, 11 12 11-34. doi:10.1002/0471250953.bi1112s47

Raudvere, U., Kolberg, L., Kuzmin, I., Arak, T., Adler, P., Peterson, H., & Vilo, J. (2019). g:Profiler: a web server for functional enrichment analysis and conversions of gene lists (2019 update). *Nucleic Acids Res, 47*(W1), W191-W198. doi:10.1093/nar/gkz369

Rhind, N., Chen, Z., Yassour, M., Thompson, D. A., Haas, B. J., Habib, N., . . . Nusbaum, C. (2011). Comparative functional genomics of the fission yeasts. *Science, 332*(6032), 930-936. doi:10.1126/science.1203357

Rutherford, K. M., Harris, M. A., Oliferenko, S., & Wood, V. (2022). JaponicusDB: rapid deployment of a model organism database for an emerging model species. *Genetics, 220*(4). doi:10.1093/genetics/iyab223

Santoni, D., Castiglione, F., & Paci, P. (2013). Identifying correlations between chromosomal proximity of genes and distance of their products in protein-protein interaction networks of yeast. *PLoS One, 8*(3), e57707.

Seeman, T. (2018). Barrnap - BAsic Rapid Ribosomal RNA Predictor (Version 0.9). Retrieved from https://github.com/tseemann/barrnap/

Shen, W., Le, S., Li, Y., & Hu, F. (2016). SeqKit: A Cross-Platform and Ultrafast Toolkit for FASTA/Q File Manipulation. *PLoS One, 11*(10), e0163962. doi:10.1371/journal.pone.0163962

Shen, X. X., Steenwyk, J. L., LaBella, A. L., Opulente, D. A., Zhou, X., Kominek, J., . . . Rokas, A. (2020). Genome-scale phylogeny and contrasting modes of genome evolution in the fungal phylum Ascomycota. *Sci Adv, 6*(45). doi:10.1126/sciadv.abd0079

Shumate, A., & Salzberg, S. L. (2020). Liftoff: accurate mapping of gene annotations. *Bioinformatics, 37*(12), 1639-1643. doi:10.1093/bioinformatics/btaa1016

Sipiczki, M., Kucsera, J., Ulaszewski, S., & Zsolt, J. (1982). Hybridization studies by crossing and protoplast fusion within the genus Schizosaccharomyces Lindner. *Microbiology, 128*(9), 1989-2000.

Slooff, W. C. (1970). Genus 6. Pityrosporum Sabouraud. *The yeasts, a taxonomic study*, 1167-1186.

Smit, A. F. A., Hubley, R., & Green, P. (2015). RepeatMasker Open-4.0. Retrieved from http://www.repeatmasker.org

Stecher, G., Tamura, K., & Kumar, S. (2020). Molecular Evolutionary Genetics Analysis (MEGA) for macOS. *Mol Biol Evol, 37*(4), 1237-1239. doi:10.1093/molbev/msz312

Sugiyama, J., Hosaka, K., & Suh, S. O. (2006). Early diverging Ascomycota: phylogenetic divergence and related evolutionary enigmas. *Mycologia, 98*(6), 996-1005. doi:10.3852/mycologia.98.6.996

Tamura, K., Battistuzzi, F. U., Billing-Ross, P., Murillo, O., Filipski, A., & Kumar, S. (2012). Estimating divergence times in large molecular phylogenies. *Proc Natl Acad Sci U S A, 109*(47), 19333-19338. doi:10.1073/pnas.1213199109

Tamura, K., Tao, Q., & Kumar, S. (2018). Theoretical Foundation of the RelTime Method for Estimating Divergence Times from Variable Evolutionary Rates. *Mol Biol Evol, 35*(7), 1770-1782. doi:10.1093/molbev/msy044

Tarailo-Graovac, M., & Chen, N. (2009). Using RepeatMasker to identify repetitive elements in genomic sequences. *Curr Protoc Bioinformatics, Chapter 4*, Unit 4 10. doi:10.1002/0471250953.bi0410s25

Teresa Avelar, A., Perfeito, L., Gordo, I., & Godinho Ferreira, M. (2013). Genome architecture is a selectable trait that can be maintained by antagonistic pleiotropy. *Nature Communications, 4*(1), 2235.

Thorvaldsdottir, H., Robinson, J. T., & Mesirov, J. P. (2013). Integrative Genomics Viewer (IGV): high-performance genomics data visualization and exploration. *Brief Bioinform, 14*(2), 178-192. doi:10.1093/bib/bbs017

Tong, P., Pidoux, A. L., Toda, N. R. T., Ard, R., Berger, H., Shukla, M., . . . Allshire, R. C. (2019). Interspecies conservation of organisation and function between nonhomologous regional centromeres. *Nat Commun, 10*(1), 2343. doi:10.1038/s41467-019-09824-4

Walker, B. J., Abeel, T., Shea, T., Priest, M., Abouelliel, A., Sakthikumar, S., . . . Earl, A. M. (2014). Pilon: an integrated tool for comprehensive microbial variant detection and genome assembly improvement. *PLoS One, 9*(11), e112963. doi:10.1371/journal.pone.0112963

Wang, N., Clark, L. D., Gao, Y., Kozlov, M. M., Shemesh, T., & Rapoport, T. A. (2021). Mechanism of membrane-curvature generation by ER-tubule shaping proteins. *Nat Commun, 12*(1), 568. doi:10.1038/s41467-020-20625-y

Wickerham, L. J., & Duprat, E. (1945). A remarkable fission yeast, Schizosaccharomyces versatilis nov. sp. *Journal of bacteriology, 50*(5), 597-607.

Wong, S., & Wolfe, K. H. (2005). Birth of a metabolic gene cluster in yeast by adaptive gene relocation. *Nat Genet, 37*(7), 777-782. doi:10.1038/ng1584

Wood, V., Gwilliam, R., Rajandream, M. A., Lyne, M., Lyne, R., Stewart, A., . . . Nurse, P. (2002). The genome sequence of Schizosaccharomyces pombe. *Nature, 415*(6874), 871-880. doi:10.1038/nature724

Wood, V., Harris, M. A., McDowall, M. D., Rutherford, K., Vaughan, B. W., Staines, D. M., . . . Oliver, S. G. (2012). PomBase: a comprehensive online resource for fission yeast. *Nucleic Acids Res, 40*(Database issue), D695-699. doi:10.1093/nar/gkr853

Yam, C., Gu, Y., & Oliferenko, S. (2013). Partitioning and remodeling of the Schizosaccharomyces japonicus mitotic nucleus require chromosome tethers. *Curr Biol, 23*(22), 2303-2310. doi:10.1016/j.cub.2013.09.057

Yam, C., He, Y., Zhang, D., Chiam, K. H., & Oliferenko, S. (2011). Divergent strategies for controlling the nuclear membrane satisfy geometric constraints during nuclear division. *Curr Biol, 21*(15), 1314-1319. doi:10.1016/j.cub.2011.06.052

Yarrow, D. (1984). Schizosaccharomyces Lindner. *The yeasts—a Taxonomic Study. Amsterdam: Elsevier Science Publishers*, 414-422.

Yates, A. D., Allen, J., Amode, R. M., Azov, A. G., Barba, M., Becerra, A., . . . Chakiachvili, M. (2022). Ensembl Genomes 2022: an expanding genome resource for non-vertebrates. *Nucleic acids research, 50*(D1), D996-D1003.

Yukawa, M., & Maki, T. (1931). Schizosaccharomyces japonicus nov. spec La Bul Sci Falkultato Terkultura Kjusu Imp Univ. *Fukuoka, Japan, 4*, 218-226.

Supplementary Data

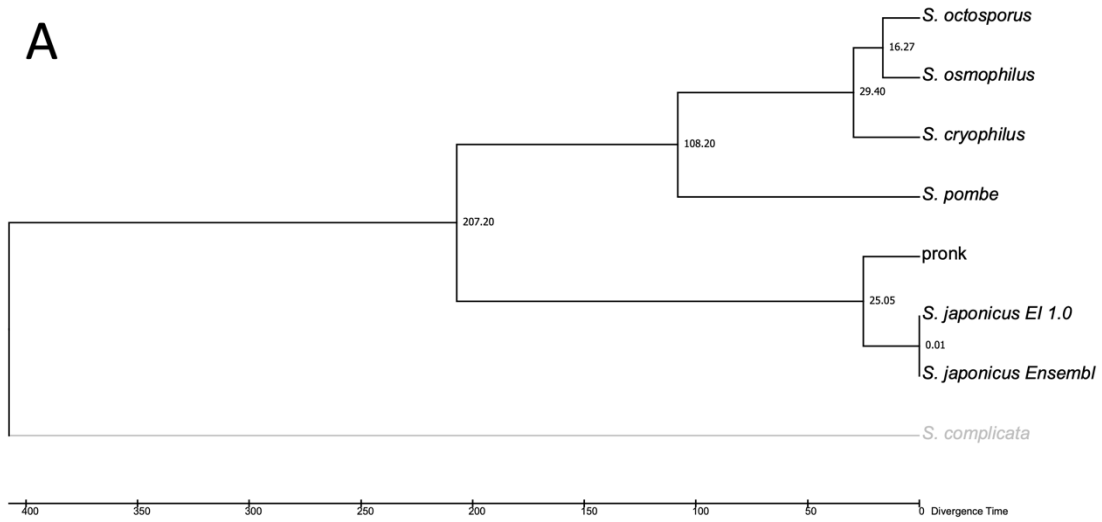

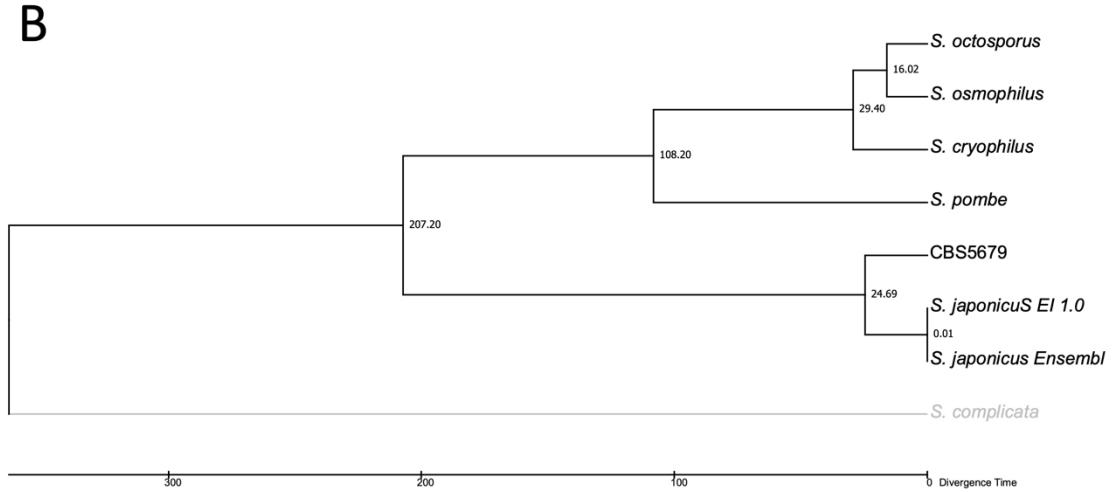

Supplementary Figure S1
Calibration of CBS5679 - *S. japonicus* split using (A) RelTree Maximum Likelihood and (B) RelTree Branch Lengths. The node numbers represent divergence times in millions of years. In the trees, the previously-calculated timing of the *S. octosporus* – *S. osmophilus* split (15.7 MYA) was removed and recalculated along with the *S. japonicus* – CBS56679 split, confirming our previously calculated divergence time of 25 MYA.

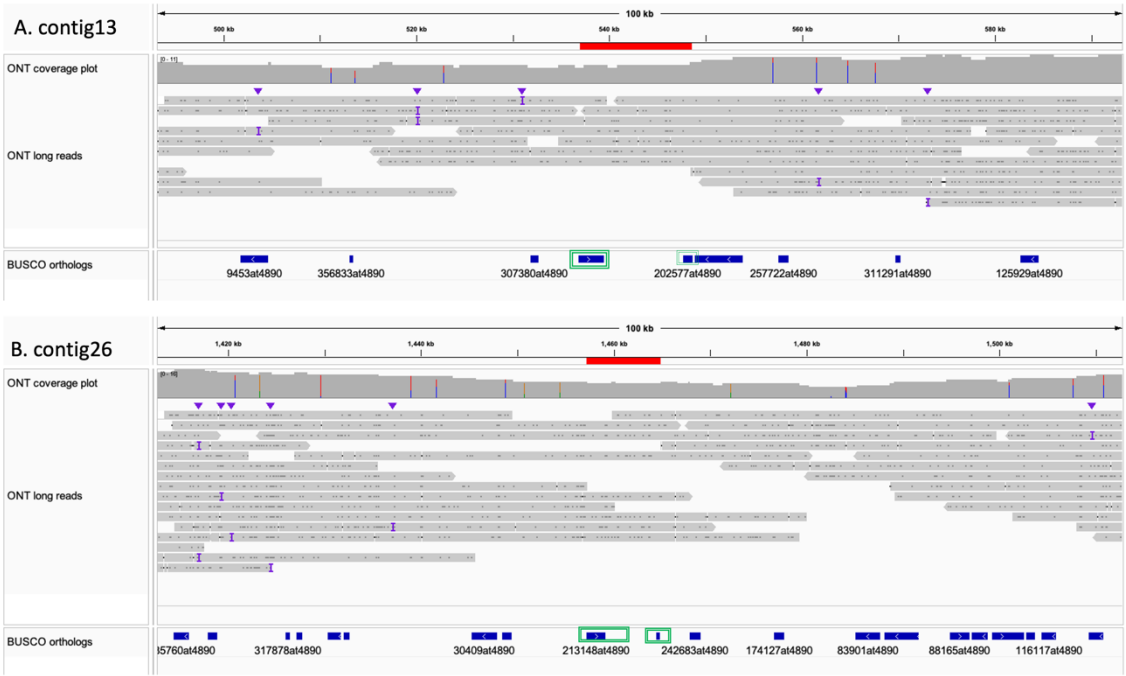

Supplementary Figure S2
Long-read (ONT) coverage across translocations on (A) contig13 and (B) contig26, using the IGV genome browser. The solid red line represents the translocations (relative to *S. japonicus* chromosomes 1 and 2), the green squares highlight the flanking BUSCO orthologs, and the grey horizontal bars in the 'ONT long reads' panel represent individual ONT reads across the translocations.

Supplementary Table S1
Co-ordinates of the BUSCO single-copy orthologs present in both CBS5679 and *S. japonicus* EI 1.0. The table is sorted by the co-ordinates of orthologs for the chromosome-scale assembly *S. japonicus* EI 1.0.

Supplementary Data S1 (s_versatilis.gff.tar.gz)
This archive contains four annotation files in GFF format:
s_versatilis_liftoff.gff – Genome annotation from Ensembl Fungi assembly of *S. japonicus* using Liftoff (Shumate & Salzberg, 2020).
s_versatilis_repeats.gff – Annotation of repeat content from RepeatModeler v2.0.3 (Flynn et al., 2020) and RepeatMasker (v4.1.2-p1) (Smit et al., 2015; Tarailo-Graovac & Chen, 2009).
s_versatilis_trnascan.gff – Annotation of tRNA loci using tRNAscan-SE (v2.0.12) (Chan et al., 2021)

s_versatilis_barrnap_rrna.gff – Annotation of rRNA loci using barrnap (v0.9) (Seeman, 2018).